Journal of Safety Science and Resilience 2 (2021) 199–207

Science Press

Contents lists available at ScienceDirect

Journal of Safety Science and Resilience

journal homepage: http://www.keaipublishing.com/en/journals/journal-of-safety-science-and-resilience/


# A multi-scale agent-based model of infectious disease transmission to assess the impact of vaccination and non-pharmaceutical interventions: The COVID-19 case

Luyao Kou [a], Xinzhi Wang [b], Yang Li [b], Xiaojing Guo [a], Hui Zhang [a,*]

[a] Institute of Public Safety Research, Tsinghua University, Beijing 100084, PR China
[b] School of Computer Engineering and Science, Shanghai University, Shanghai 200444, PR China

ARTICLE INFO

*Keywords:*
Public health
Transmission risk
Agent-based model
Epidemic simulation
Policy assessment

ABSTRACT

Mathematical and computational models are useful tools for virtual policy experiments on infectious disease control. Most models fail to provide flexible and rapid simulation of various epidemic scenarios for policy assessment. This paper establishes a multi-scale agent-based model to investigate the infectious disease propagation between cities and within a city using the knowledge from person-to-person transmission. In the model, the contact and infection of individuals at the micro scale where an agent represents a person provide insights for the interactions of agents at the meso scale where an agent refers to hundreds of individuals. Four cities with frequent population movements in China are taken as an example and actual data on traffic patterns and demographic parameters are adopted. The scenarios for dynamic propagation of infectious disease with no external measures are compared versus the scenarios with vaccination and non-pharmaceutical interventions. The model predicts that the peak of infections will decline by 67.37% with 80% vaccination rate, compared to a drop of 89.56% when isolation and quarantine measures are also in place. The results highlight the importance of controlling the source of infection by isolation and quarantine throughout the epidemic. We also study the effect when cities implement inconsistent public health interventions, which is common in practical situations. Based on our results, the model can be applied to COVID-19 and other infectious diseases according to the various needs of government agencies.

## 1. Introduction

The COVID-19 pandemic is caused by a novel coronavirus identified in December 2019. Since 2021, variants of this virus have emerged or become dominant in many countries, with Delta variant being the most transmissible. Over 68% of COVID-19 infections in the majority of European countries and the US are Delta variant. As of 18 August 2021, more than 209 million cases and 4.38 million deaths have been reported, making it one of the world's deadliest pandemics to date [1]. To curb disease propagation, non-pharmaceutical interventions (NPIs) have been implemented to various degrees across the world and major efforts have been taken to develop effective vaccines. The uncertain situation requires a flexible model of infectious disease transmission to understand the future trajectory of this disease and to analyze the efficacy of vaccination and possible NPIs, which would provide the authorities with practical recommendations on disease control [2].

Infectious disease transmission models are generally one of these approaches that we refer to here as statistical model, equation-based model, and agent-based model. Statistical model adopts historical data and uses machine learning and regression methods to predict short-term disease spread [3] or mine the relationship between aggregate variables, for example population movements and the infections [4,5]. However, without specifying the causal connections between these variables, it is hard for these models to predict the epidemiological dynamics (such as time to peak and whether the resurgence will occur) or to evaluate the effect of possible interventions.

Equation-based model provides a theoretical framework for epidemiological analyses to project how infectious diseases progress in a population. A classical model is SIR (Susceptible-infected-removed) presented by Kermack and Mckendrick [6]. Complicated equation-based models are gradually proposed considering vaccine [7], quarantine [8,9], dynamic transmission rate [10], diversity of population [11], and other important factors in epidemic spreading. Most recently, Peixoto et al.[12] integrated mobility data into the disease spread between locations, while the transmission within each location is modeled as a SI model. Although equation-based models are proper for simulating large-scale behaviors of a pandemic, they often fail to explain social phenomena associated with individual interactions. Furthermore, different interventions such as wearing masks and social distancing take effect through only one

* Corresponding author.
*E-mail address:* zhhui@mail.tsinghua.edu.cn (H. Zhang).

https://doi.org/10.1016/j.jnlssr.2021.08.005
Received 18 August 2021; Accepted 20 August 2021

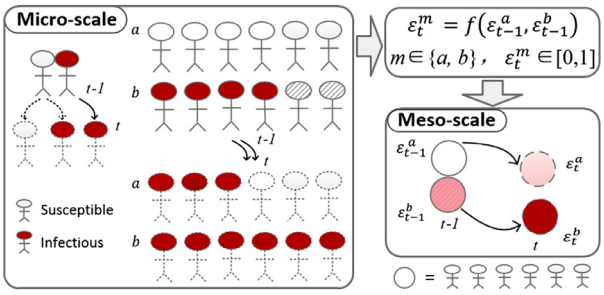


**Fig. 1.** Schematic diagram of MSABM.

parameter like the transmission rate in the SIR-like model. These concerns limit their utility in investigating public health interventions at a finer resolution and providing specific and targeted suggestions.

Agent-based model is an increasingly popular method for visualizing and informing such a complex dynamic system in public health, as the model can capture the interactive, spatial, heterogeneous, and local characteristics of the epidemic spreading [13]. Various agent-based models have been used to investigate the COVID-19 transmission dynamics [14]. Bouchnita and Jebrane [15] considered relaxed and strict control measures in a close region of 250 individuals. Silva et al. [16] analyzed seven different scenarios of social distancing interventions with varying epidemiological and economic effects. They considered combining the use of face masks and partial isolation as a practicable approach. The flexibility of the agent-based model enables its application to different topics such as university campus [31], facilities [17], and hospitals [18]. However, agent-based models generally require a long simulation time due to a large number of independent individuals and the complexity of models when applied to disease spread in cities and countries. It is unpractical using such a model to run multiple simulations of various scenarios especially in an uncertain situation where a previously unknown virus or a new variant strikes.

In this paper, we propose a multi-scale agent-based model (MSABM) for disease spread between cities and within a city. The degree of freedom of the model is reduced using the knowledge of person-to-person transmission without losing the significant complexity of the agent-based model. At the micro scale, an agent represents a person while at the meso scale an agents refers to hundreds of individuals. The micro-scale contact and infection of individuals provide insights for the meso-scale interactions of agents. The MSABM has advantages over traditional methods. First, this model requires less computational resources and shorter execution time which improves the efficiency of simulations over a large area. Second, the heterogeneity is incorporated into the model through defining each agent individually with its own profile of infection and mobility. Third, the easiness for visualization of our approach helps exhibit the evolution of complex dynamic systems, especially when some phenomena are counterintuitive. Fourth, the model is highly flexible as it contains relatively more adjustable parameters compared to classical mathematical models. It thus allows the design of what-if scenarios that consider vaccination and different types of NPIs, through modifying the simulation parameters and observing the population outcomes.

The paper is organized as follows. Section 2 describes the proposed model. Section 3 presents the results and discussions. Finally, conclusions are drawn in Section 4.

## 2. The multi-scale agent-based model (MSABM) of infectious disease transmission

This article aims to simulate the agent-based spreading of infectious diseases using the knowledge from person-to-person transmission. Fig. 1 provides the schematic diagram of the proposed model. At the micro scale, the pattern of infection is relatively straightforward. A susceptible individual can either stay healthy or be infected after its contact with an infectious individual. At the meso scale, an agent represents hundreds or thousands of individuals in the scenarios where virus spreads in a large area like cities or countries. The similarity in the pattern of infection for the two scales allows us to construct the meso-scale disease transmission between agents with the law extracted from the micro scale. Specifically, the interactions of agents at the meso scale can be related to the contact and infection of individuals at the micro scale. This section is divided into three parts, that is, parameters and initialization, behavioral rules, and computational process to present and describe the MSABM for disease propagation in detail. The total framework of the paper is depicted in Fig. 2.

### 2.1. Parameter and initialization

In this sub-section, we first describe four important parameters of the model. Then the consideration of individual differences and agent initialization are introduced.

1) *Probabilityofbeinginfected*, $\eta$: At the micro scale, the probability of a close contact being infected is considered through the use of parameter $\eta$. This probability depends on several factors such as one's health condition, personal protection measures, and vaccination. Value of $\eta$ ranges from 0 to 1. A smaller $\eta$ represents a lower probability of infection. It is assumed that vaccine could provide perfect protection to a proportion (vaccine efficacy, $ve$) of individuals who receive it, and $\eta$ of these individuals equals to zero.
2) *Infectionproportionofagenta*, $\varepsilon_t^a$: At the meso scale, suppose that an agent indicates $i$ individuals. The parameter $\varepsilon_t^a$ that ranges from 0 to 1 is used to denote the infection proportion of agent $a$ at time $t$. For example, $\varepsilon_t^a$ equals to $1/i$ if one individual related to agent $a$ is infected. The value of $\varepsilon_t^a$ depends on the previous state of agent $a$ and agent $b$ in contact with it (that is, $\varepsilon_{t-1}^a$ and $\varepsilon_{t-1}^b$) and can be expresses as

$$\varepsilon_t^a = m * \varepsilon_{t-1}^b + n * \varepsilon_{t-1}^a + k, \tag{1}$$

where the weights $(m, n)$ and biases $(k)$ are obtained through linear regression of multiple simulation results at the micro scale. Considering the effect of vaccination, the range of infection proportion is limited to below 1-$vr$*$ve$ where $vr$ and $ve$ denote the vaccination rate and vaccine efficacy respectively.
3) *Characteristicsofmovement*, $v$: The infection maintains a close association with population movements. $v$ summarizes several factors that affect the mobility of a person such as commuting to work, attending school, and purchase of necessities. With $v$ it is possible to simulate the distinct class of agents. $v$ can be the same for groups of agents, for example, people with the same pace of life such as work schedule. Furthermore, factors difficult to describe such as entertainment needs and temporary business trips, alter this parameter and present the individual heterogeneity. In the model, population is divided into three types, floating population ($v_1$), permanent working population ($v_2$), and permanent non-working population ($v_3$). The moving speed $v$ varies for different types of population.
4) *Efficiencyofisolationandstrengthofquarantine*, $\gamma$: Isolation is the act of separating an infectious patient from healthy individuals in order to protect the general public from exposure of a contagious disease [19]. Various approaches of isolation exist such as isolation in hospitals or temporal facilities, and self-isolation in situations when medical resources are insufficient. Different from isolation, quarantine separates and restricts the movement of close contacts, people who might have been exposed to a contagious disease [20]. The parameter $\gamma$ is used to quantify the efficiency of isolation and strength of quarantine. For example, if $\gamma_i$ for agent $i$ is 0.7, when its proportion of infections ($\varepsilon_t^i$) equals to or is larger than 0.7 the agent is unable to interact with other agents and $\varepsilon_t^i$ of this agent stops rising.

Individual differences are considered for a more realistic simulation.

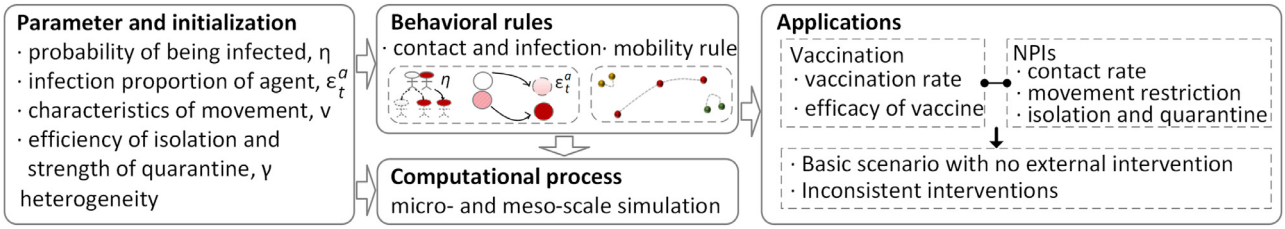


**Fig. 2.** Framework of multi-scale agent-based infectious disease transmission.

- For each individual, it is assigned a probability of infection $\eta$ which is randomly set with values uniformly distributed between the defined lower and upper limits ($[l_\eta, u_\eta]$). Values close to $l_\eta$ denotes people in good health or people that take proper protection measures. Values close to $u_\eta$ refer to people at higher risk of infection.
- As for the moving speed, the lower and upper limits ($[l_v, u_v]$) are set for each type of population. Values close to $u_v$ represent agents with high movement speed and mobility, while values close to $l_v$ denote poor mobility.
- The model also emphasizes the heterogeneity in the efficiency of isolation and strength of quarantine. For each agent, $\gamma_i$ is sampled from chi-square-like distribution with expectation $\gamma$ and variance $0.2^*\gamma$, as in practice there exist occasions when individuals or groups are isolated after being infected for a long time.

An agent is represented as $\mathbf{a}_{ij}^g$ in the agent-based model. $i$ denotes the type of population that is related to agents' movement behaviors which are described in Section 2.2. $g$ is the location tag, indicating the city to which the agent belongs. The agents of the same population type $i$ inside the city $g$ are numbered with $j$. In the first iteration ($t = 1$), the location of each agent is initialized randomly in a two-dimensional space. Each coordinate $\mathbf{a}_{ij,d}^g$ ($d \in \{x, y\}$) is determined with a value uniformly distributed between the upper $U_d^g$ and lower $L_d^g$ boundaries of the city, expressed as

$$\mathbf{a}_{ij,d}^g(1) = L_d^g + rand(0,1)(U_d^g - L_d^g), \tag{2}$$

where $rand(0, 1)$ function provides a random value between zero and one within a uniform distribution.

### 2.2. Behavioral rules

To simulate disease transmission dynamics, agents update their states and locations characterized by simple rules and interactive behaviors. In this process, agents observe contact and infection rule to determine whether being infected. Mobility rule guides the movement behavior of agents.

1) *Contact and infection*: For each collision between two agents, the validity of collision is determined firstly for the micro and meso scale. A random number is generated within a uniform distribution $\mathbf{U}[0, 1]$. If the number is less than or equals to the contact rate denoted as $\sigma$, the two agents contact and they can influence each other.
   At the micro scale, a similar probabilistic process as above is conducted to determine whether the susceptible individual will be infected by the infectious one in contact with it. If the random number is less than or equals to the susceptibility $\eta$ of the individual, it is infected, otherwise, it stays healthy in spite of the contact. At the meso scale, the infection proportion $\varepsilon$ of the two agents in contact changes according to Eq. (1).
2) *Mobility rule*: At the meso scale, the model selects the motion path for each agent through a probabilistic decision process. Under this process, a random number is generated within a uniform distributed $\mathbf{U}[0, 1]$. If the number is less than or equals to the predefined percentage of floating population $Per_f$, the agent flows between city; otherwise, it moves inside the city. Then for permanent population, whether it belongs to working population or non-working residents is determined through a similar probabilistic process. The generated random number is compared with the percentage of working population $Per_l$.

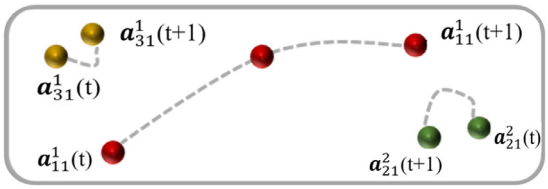


**Fig. 3.** Mobility behavior. For agent $\mathbf{a}_{ij}^g(t)$, $t$ denotes time step; $i$ indicates the type of population including floating population ($i = 1$), permanent working residents ($i = 2$), and non-working population ($i = 3$); $g$ represents the city to which the agent belongs($g = \{1, 2\}$ in the case shown in this figure).

The floating population flows between cities to meet the needs of business trips, medical treatment, family visits, etc. $Per_{ij}$ represents the percentage of population that moves from city $i$ to $j$. Floating population moves along a fixed route between two cities and stays in the target city for a period of time before moving back.

The permanent population moves within the city, usually for the purpose of commuting to work and purchasing daily necessities. The activity range of the permanent population is the boundary of the city to which it belongs, given by

$$\mathbf{a}_{ij,d}^g(t+1) = \mathbf{a}_{ij,d}^g(t) + rand(-1,1)v_i, \tag{3}$$

where $i$ indicates working residents ($i = 2$) and non-working population ($i = 3$). $rand(-1, 1)$ delivers a random number between $-1$ and 1. The moving speed $v_i$ varies for different types of population. For example, the speed of non-working population may be much lower, as they avoid unnecessary activities to reduce the risk of infection. Fig. 3 illustrates the rule of mobility.

### 2.3. Computational process

The model for disease propagation is employed as an iterative process that considers parameter initialization and behavioral rules. Algorithms 1 and 2 present the multi-scale model in the form of pseudocode.

An agent represents an individual at the micro scale, while an agent denotes more than one individual at the meso scale. The micro-scale simulation aims to provide the correlation between the infection proportion at current iteration ($\varepsilon_t^a$) and the proportion at the previous iteration ($\varepsilon_{t-1}^a, \varepsilon_{t-1}^b$) for the meso-scale simulation, as shown in Eq. (1).To do that, half of the individuals are labeled as $a$ and the others are marked as $b$ at the micro scale. We run multiple simulations with different initial infection proportion of $a$ and $b$. The weights $(m, n)$ and biases $(k)$ of Eq. (1) are then obtained through linear regression of these multiple simulation results, as shown in Algorithm 1, line 14.

At the micro scale, the predefined lower and upper infection probability range $[l_\eta, u_\eta]$, vaccine rate $vr$, and vaccine efficacy $ve$ are used to initialize the susceptible of each agent. The focus of this scale is the

**Algorithm 1:** The micro-scale simulation.

1 **repeat**
  **Input:** $\varepsilon_1^a, \varepsilon_1^b, \sigma, [l_\eta, u_\eta], vr, ve, Per_l, [L_d^1, U_d^1]$
2  **function** Initialization**for** *each agent* $\mathbf{a}_{ij}^1$ **do**
3  $\eta \leftarrow$ Initialize Susceptibility($[l_\eta, u_\eta]$, $vr$, $ve$);
4  $v \leftarrow$ Initialize Mobility($Per_l, [l_v, u_v]$);
5  $\sigma \leftarrow$ Initialize ContactRate;
6  $\mathbf{a}_{ij,d}^1 \leftarrow$ Initialize Position($[L_d^1, U_d^1]$);
7  **end functionrepeat**
8  **function** Contact & Infection($\sigma, \eta$);
9  **function** Mobility($v$);
10  **until** $t >$ *maximum simulation iterations*;
  **Output:** $\varepsilon_t^a, \varepsilon_t^b$
11 **until** *the number of multiple runs reached*;
12 **function** Linear Regression($\varepsilon_t^a, \varepsilon_{t-1}^b, \varepsilon_{t-1}^b$)**Output:** $m, n, k$

**Algorithm 2:** The meso-scale simulation.

  **Input:** $\gamma, \sigma, m, n, k, Per_f, Per_l, [l_v, u_v], Per_{ij}, [L_d^g, U_d^g]$
1 **function** Initialization**for** *each agent* $\mathbf{a}_{ij}^g$ **do**
2  $v \leftarrow$ Initialize Mobility($Per_f, Per_l, [l_v, u_v]$);
3  $\sigma \leftarrow$ Initialize ContactRate;
4  $\gamma \leftarrow$ Initialize Isolation&QuarantineStrength;
5  $\mathbf{a}_{ij,d}^g \leftarrow$ Initialize Position($[L_d^g, U_d^g]$);
6 **end functionrepeat**
7  **function** Contact & Infection($\sigma, m, n, k, vr, ve$);
8  **function** Mobility($v$, $Per_{ij}$);
9  **function** Isolation & Quarantine($\gamma$);
10 **until** $t >$ *maximum simulation iterations*;
  **Output**: infection proportion of each city

contacts between individuals, and cross-city movements are not considered. Individuals are located at one city and their positions are initialized as shown in line 7. The fraction of working population $Per_l$ and the predefined lower and upper moving speed $[l_v, u_v]$ are employed to characterize the mobility of individuals (line 5).

At the meso scale, the proportion of floating population $Per_f$ and working residents $Per_l$, and the range $[l_v, u_v]$ are used to initialize the moving speed of agents. The rule of mobility is conducted independently for each agent (Algorithm 2, line 10). The infection pattern extracted from micro simulation guides the changes in infection proportion of agents (line 9). When the infection proportion $\varepsilon$ of an agent equals to or is larger than the value of $\gamma$ for this agent, it is unable to interact with other agents and its $\varepsilon$ stops rising (line 11). The states and locations of agents are updated every frame, until the maximum number of simulation iterations is reached. The infection proportion of agents per iteration in each city acts as output data. The Unity plantform [21] and C# program are employed to implement the simulations described in this paper. Snapshots of meso-scale simulation using the model are provided in Fig. 4.

## 3. Results and discussion

The model is flexible and enables testing of scenarios considering different strategies of vaccination and NPIs. This section shows the characteristics of the proposed model and the results that it can provide.

### 3.1. Study area and data setting

In our approach the infectious disease transmission is simulated using the census and mobility data of four important cities, that is, Shanghai, Hangzhou, Nanjing, and Hefei in China's Yangtze River Delta Economic Zone. The number of permanent and floating population as well as the percentage of working (between 15 and 64 years old) and non-working residents are obtained from China statistical yearbook 2019 [22]. The census data is shown in Table 1. It is assumed that a floating agent stays in a city for about two days before moving to other cities. The proportion of agents moving from one city to other cities is extracted from Baidu Migration Platform [23], as shown in Table 2.

The moving speed differs for floating individuals, working-age adults, and the non-working population. These values are obtained through calculating the actual moving speed. On average, people spend 28 min on commuting and move 9.18 km in China [24]. The speed of the working population is thus 0.33 kilometers per minute. The non-working population usually moves by foot with the speed of 0.08 kilometers per minute [25]. The floating population tend to drive or take the high-speed rail, the speed of which is about 1.13 kilometers per minute.

### 3.2. Infection pattern extracted from micro simulation

Since there are a large population under voluntary home isolation, it is assumed that 1.78% of the total population (about 963,200 people) in our study area may be affected by the epidemic. Value of this percentage refers to the article that simulates the transmission dynamics in Wuhan, China [26]. The total population is used when calculating the infection proportion of a city in the following sections. The number of agents at the meso scale is set to 1120, and an agent represents 860 individuals. The micro-scale simulation aims to provide the contact and infection pattern of two agents at the meso scale. Therefore, the micro scale considers a population of 1720 individuals. The weights $(m, n)$ and biases $(k)$ of Eq. (1) are obtained through linear regression of multiple simulation results at the micro scale.

The coefficients of linear regression equation are shown in Fig. 5. Five cases are adopted with varying vaccination rate and contact rate. Fig. 5 shows that with the increasing strength of interventions from case I to V, the value of $n$ increases while the value of the other two coefficients $m$ and $k$ decreases. It shows that with the enhancement of measures the infection proportion of agents at the current time depends more on its own state at the previous iteration. For example, the equations for case I and II are as follows:

$$\begin{aligned} \varepsilon_t^a &= 0.0309 * \varepsilon_{t-1}^b + 0.9744 * \varepsilon_{t-1}^a + 0.0210, \\ \varepsilon_t^a &= 0.0220 * \varepsilon_{t-1}^b + 0.9844 * \varepsilon_{t-1}^a + 0.0129. \end{aligned} \tag{4}$$

For the same $\varepsilon_{t-1}^b$ and $\varepsilon_{t-1}^a$, the value of $\varepsilon_t^a$ in case II is smaller than that in case I. It suggests that the stricter intervention will lead to a smaller increase in the proportion of infections for an agent. The infection pattern extracted from the micro simulations is in line with our intuition that vigorous interventions can reduce the number of people infected by the virus.

### 3.3. Transmission dynamics in the absence of governmental interventions

In this basic scenario, the model is tested when the first infected person occurs in Shanghai which is a national center for commerce, trade, and transportation. The value of parameters is listed in Table 3. The lower $(l_\eta)$ and upper $(u_\eta)$ limits of the infection probability are set to 0.15 and 0.25, as the average probability of infection is 0.2 [17,27]. Similarly, the lower $(l_v)$ and upper $(u_v)$ limits of the moving speed are set as a realistic interval considering the actual moving speed.

Fig. 6 exhibits the variability in the proportion of infected people as a function of iterations. Each simulation is executed repeatedly five times considering the stochastic scheme of agent-based models. The model predicts that, in the absence of control interventions, the disease will infect 1.73% of the total population by the time of simulation. As for the four cities, the worst-hit place is Shanghai which has the largest population and the most frequent population movements. From the figure we can conclude that time to the rapid growth of infections is positively correlated with the index of population inflow from Shanghai where the

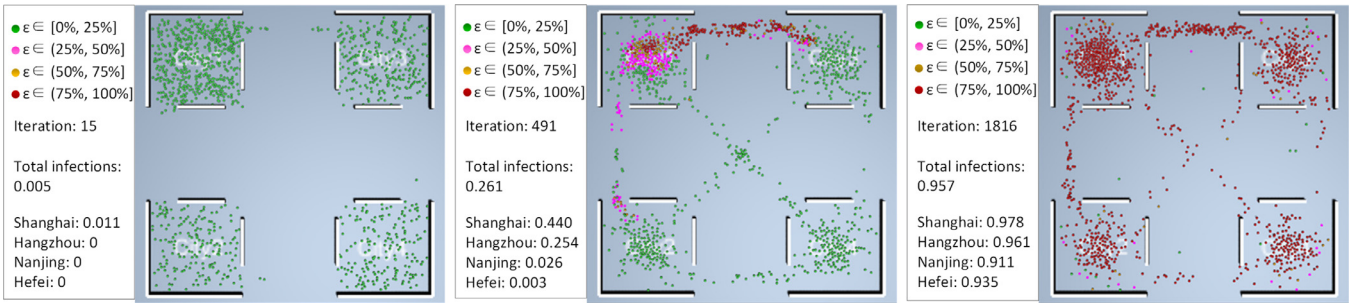


**Fig. 4.** Snapshots of meso-scale simulation using the MSABM model. $\varepsilon$ denotes the infection proportion of an agent.

**Table 1**
The number of three types of agents for COVID-19 simulation.

| City | Working-age residents | Non-working residents | Floating population |
|---|---|---|---|
| Shanghai | 213 | 87 | 200 |
| Hangzhou | 114 | 46 | 100 |
| Nanjing | 100 | 40 | 40 |
| Hefei | 100 | 40 | 40 |

**Table 2**
The proportion of movements between four cities.

| | Shanghai | Hangzhou | Nanjing | Hefei |
|---|---|---|---|---|
| Shanghai | / | 4.5% | 1.85% | 1.35% |
| Hangzhou | 4.03% | / | 0.84% | 0.64% |
| Nanjing | 2.55% | 1.14% | / | 2.06% |
| Hefei | 2.81% | 1.21% | 2.44% | / |

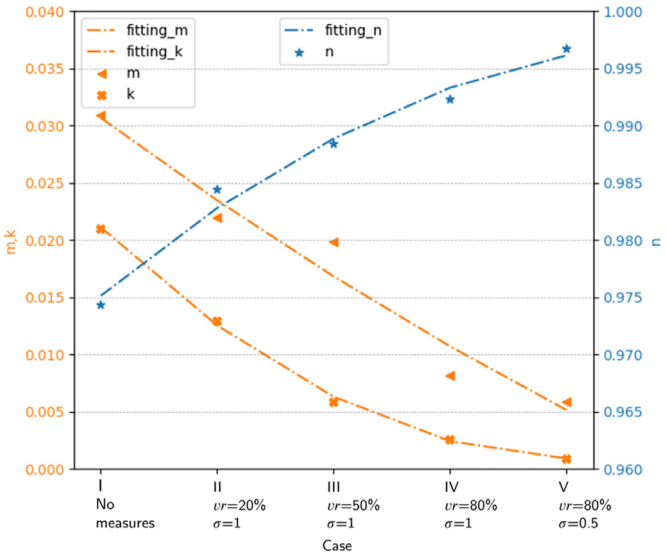


**Fig. 5.** The coefficient of linear regression equation under different cases. $vr$: vaccination rate. $\sigma$: contact rate.

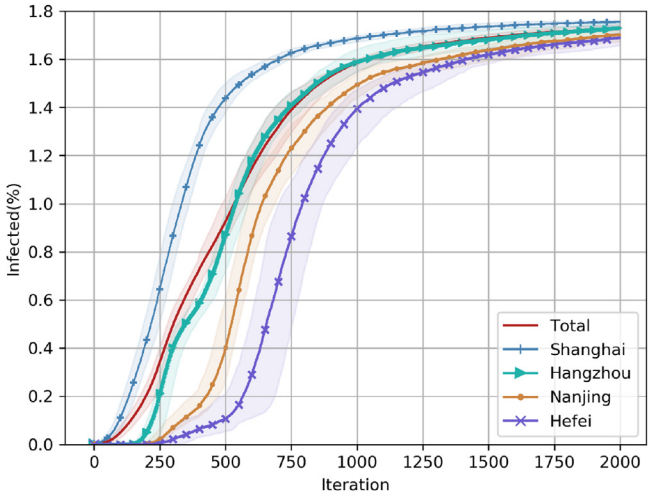


**Fig. 6.** Variability in the proportion of infected people in four cities with no external intervention on disease propagation.

disease starts in our simulation. This result corresponds with the actual COVID-19 transmission process [28].

### 3.4. Isolation and quarantine

Isolation and quarantine act as infection prevention practices used to protect the public from disease, especially in a community-wide outbreak like COVID-19. For agent $i$, $\gamma_i$ is sampled from chi-square-like dis-

**Table 3**
Default values of parameters used for COVID-19 simulation.

| Symbol | Meaning | Value |
|---|---|---|
| $\sigma$ | contact rate | 1 |
| $[l_\eta, u_\eta]$ | range of susceptibility | [0.15, 0.25] |
| $[l_{v_1}, u_{v_1}]$ | range of moving speed for floating population | [0.85, 1.41] |
| $[l_{v_2}, u_{v_2}]$ | range of moving speed for the permanent working population | [0.25, 0.41] |
| $[l_{v_3}, u_{v_3}]$ | range of moving speed for permanent non-working residents | [0.06, 0.10] |
| $Per_f$ | percentage of the floating population | Table 1 |
| $Per_l$ | percentage of the working population in permanent residents | 0.71 |
| $Per_{ij}$ | proportion of population moving from city $i$ to city $j$ | Table 2 |

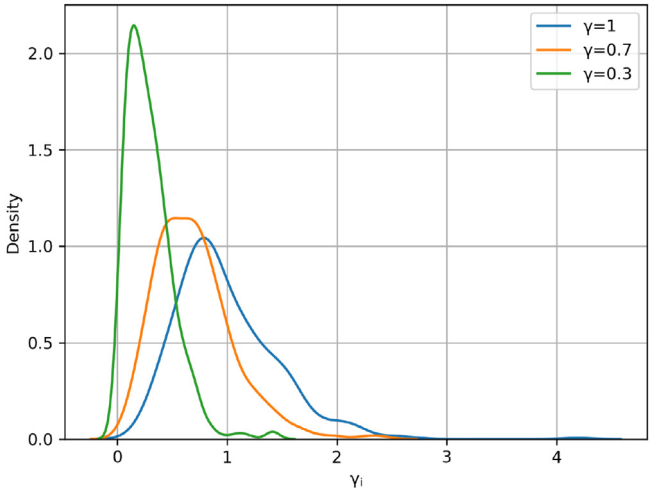


**Fig. 7.** Chi-square-like distributions with different values of $\gamma$ that represents the efficiency of isolation and strength of quarantine. The smaller value of $\gamma$ refers to the stricter isolation and quarantine measure.

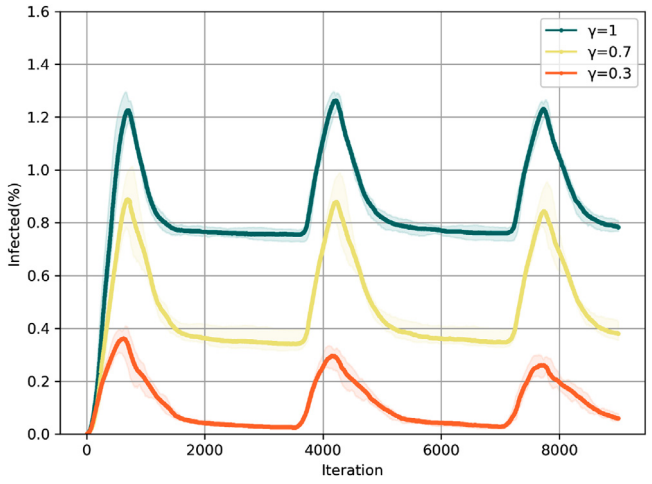


**Fig. 8.** Disease propagation with different efficiency of isolation and strength of quarantine measures. A smaller value of $\gamma$ denotes a more timely isolation of infectious individuals and a more extensive quarantine of close contacts.

tribution with expectation $\gamma$, as in practice there exist occasions when individuals or groups are isolated after being infected for a long time. The shape of chi-square-like distribution when $\gamma$ equals to 1, 0.7, and 0.3 is shown in Fig. 7.

Fig. 8 shows the effects of isolation and quarantine measures on disease propagation with different values of $\gamma$. The duration of isolation and quarantine is set to 500 iterations in the model. When $\gamma$ is set to 1, the peak of the first outbreak is reached at iteration 923. At this time, the fraction of infected individuals reaches 1.20%. When $\gamma$ equals to 0.3 the three peaks exhibits a downward trend which do not occur in the other two scenarios. In other words, the second peak is smaller than the former one, and this is also the case for the third peak. Therefore, governments and hospitals should isolate the patients and quarantine the close contacts before 30% of people in a community are infected by the virus in order to curb the disease propagation. Researches show that the memory of immune systems lasts for at least six months after infections [29]. In order to facilitate calculations, the duration of immunity is set to 2 months in our simulations in the following sections. It can be seen from Fig. 9, the number of outbreaks is negatively correlated with the duration of immunity. The model predicts two waves of the epidemic during the simulation time when the duration of immunity is taken to be 3 months.

### 3.5. Vaccination

Effective and sufficient vaccination is one of the most important measures against COVID-19. However, it will be hard to accomplish when the immunity response is imperfect (WHO requires a cutoff of 50% efficacy to approve a COVID-19 vaccine) or when the supply constraints and other factors limit the vaccination rate. The model is extended to consider the impact of vaccination. As vaccine efficacy ($ve$) can be below 100%, it is assumed that the vaccine provides perfect protection to a proportion $ve$ of individuals who receive it.

Fig. 10 demonstrates the transmission dynamics based on different vaccination rate. It is shown that with increasing vaccination rate the size of the infected population decreases. For example, when 80% of the population are vaccinated (Fig. 10D), the peak of infections declines by 67.37% compared with no vaccination (Fig. 10A). From Fig. 10D more than 0.25% of the population are infected with the virus during the plateau (e.g., from iteration 2000 to 4000 approximately). The results suggests that controlling the source of infection through isolation and quarantine interventions is an essential way to further reduce the infections and flatten the curve. From Fig. 11, the model predicts a drop of 89.56% with 80% vaccination rate and $\gamma$ equaling to 0.3 when compared to the situation shown in Fig. 10A.

### 3.6. Medium-term infectious disease propagation and the deployment of NPIs

The medium-term dynamic effect of NPIs deployment is explored in this sub-section. In our simulation, the movements of floating population are reduced by 20% and the contact rate is set to 0.5 which is half of its original value (in agreement with elementary scales of social distancing in Rothwell. [30]). The isolation and quarantine parameter $\gamma$ is set to 0.3 throughout the epidemic as it is important to control the source of infection. It is assumed that 80% of the population are vaccinated.

The adoption of NPIs decreases the risk of person-to-person transmission, especially when NPIs are implemented continuously. The figure shows the dynamics of virus transmission, assuming single periods of NPIs lasting from months 1 to 3 (Fig. 12A) or 1 to 4 (Fig. 12C), and two shorter periods during months 1 to 3 and 5.5 to 6.5 (Fig. 12B). In Fig. 12B, the additional implementation of NPIs during months 5.5 to 6.5 leads to a lower value of the third peak when compared to the scenario shown in Fig. 12A. As can be seen from Fig. 12B and C, the separate adoption of four-month NPIs causes more infections than the continuous adoption of NPIs. The proportion of infections will increase when the measures ease and then declines due to the effect of isolation and quarantine interventions. Quantification of the impact of NPIs deployment is helpful to give the government a reference in order to make an effective and dynamic emergency plan to curb infectious disease propagation.

### 3.7. Inconsistent interventions

Simulations in previous sections assume that all cities implement the same interventions consistently. This section studies the impact when cities take different and inconsistent measures against COVID-19. To do that two cases I and II are simulated. For both cases, simulations for cities are executed through adopting the following parameter settings, that is, contact rate $\sigma$, the parameter of isolation and quarantine $\gamma$, and vaccination rate equal to 0.5, 0.3, and 80% respectively, except for Hangzhou in case II that maintains the same parameters as the basic scenario with no governmental interventions in Section 3.3.

Fig. 13 and Table 4 show the simulated results of the two cases. As can be seen there are more infected agents in case II than in case I. In case II, Hangzhou that does not take stringent measures as other

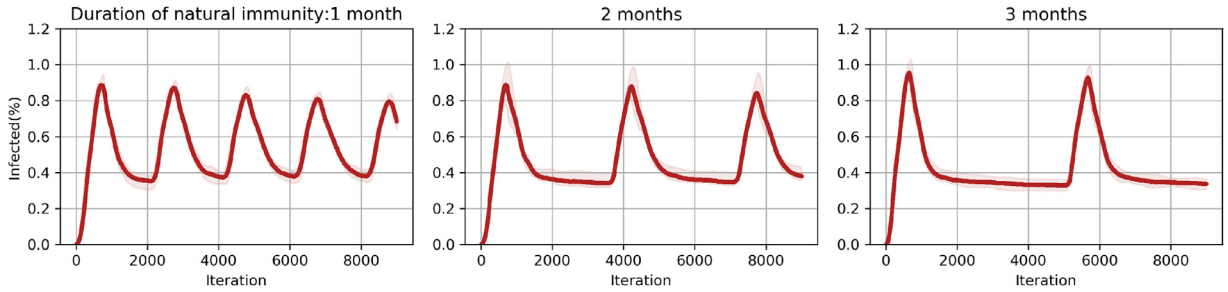


**Fig. 9.** The effects of duration of immunity on disease transmission dynamics ($\gamma = 0.7$ is assumed in all the cases).

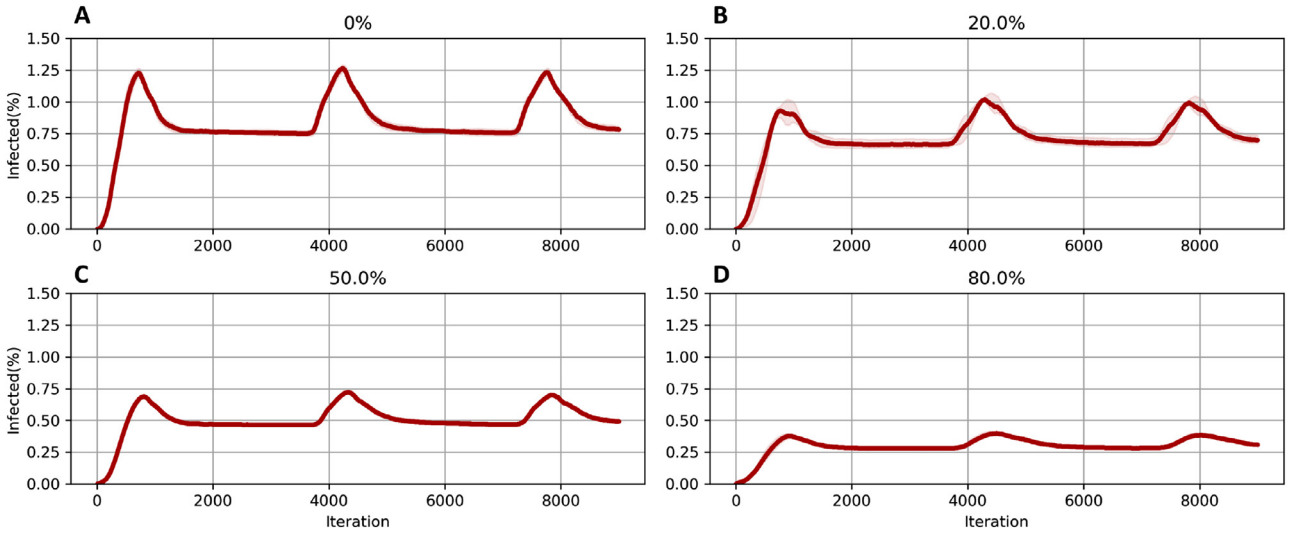


**Fig. 10.** Infectious disease propagation with different vaccination rate ($\gamma = 1$ and $ve = 0.8$ are assumed in all the cases).

**Table 4**
The values of the first and second peak and the corresponding number of iterations for case I and II.

| Peak | Case | Total value (iteration) | Shanghai | Hangzhou | Nanjing | Hefei |
|---|---|---|---|---|---|---|
| the first peak (iteration) | case I | 0.0943 (1491) | 0.1024 (1444) | 0.1023 (1535) | 0.0866 (1662) | 0.0882 (1956) |
| | case II | 0.2118 (1496) | 0.1041 (1096) | / | 0.0926 (1652) | 0.0955 (1880) |
| the second peak (iteration) | case I | 0.0704 (5655) | 0.0753 (5414) | 0.0788 (5658) | 0.0683 (5836) | 0.0699 (5926) |
| | case II | 0.1998 (5182) | 0.0761 (4985) | 0.6402 (5489) | 0.0712 (5807) | 0.0679 (5904) |

cities account for the majority of infections. The fraction of infected individuals in the other three cities also increases when compared to case I. It takes less time for the cities other than Hangzhou in Case II to reach the first and second peak. The virus takes root in one city and then spreads into other cities through the inextricable connections between them. The model illustrates that regional coordination and collaboration are important to control the spread of a virus that crosses boundaries with ease.

## 4. Conclusion

The virus's delta variant drives COVID-19 surge and becomes dominant in many countries like the US, the UK, India, and China. Under such an uncertain situation, a flexible and rapid model of infectious disease transmission is needed to investigate the medium-term propagation of the epidemic and the efficacy of governmental interventions including vaccination and NPIs. This paper proposes a multi-scale agent-based model (MSABM) to explore the spread of infectious disease between cities and within a city under different scenarios. In the model, the interaction pattern of agents at the meso scale stems from the contact and infection of individuals at the micro scale. The degree of freedom of the agent-based model is thus reduced without losing the significant complexity of the model, e.g., the consideration of cross-city mobility in our model. Census and traffic data of four interdependent cities (Shanghai, Hangzhou, Nanjing, and Hefei) in China are adopted.

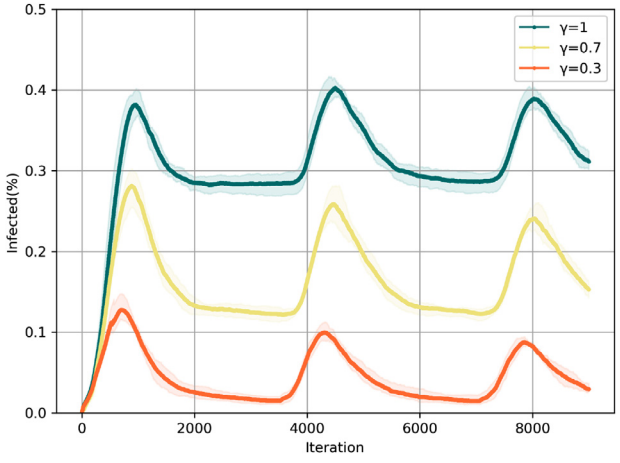


**Fig. 11.** Infectious disease propagation with different values of $\gamma$ when 80% of population has been vaccinated with vaccine efficacy 80%. $\gamma$ represents the strength of isolation and quarantine.

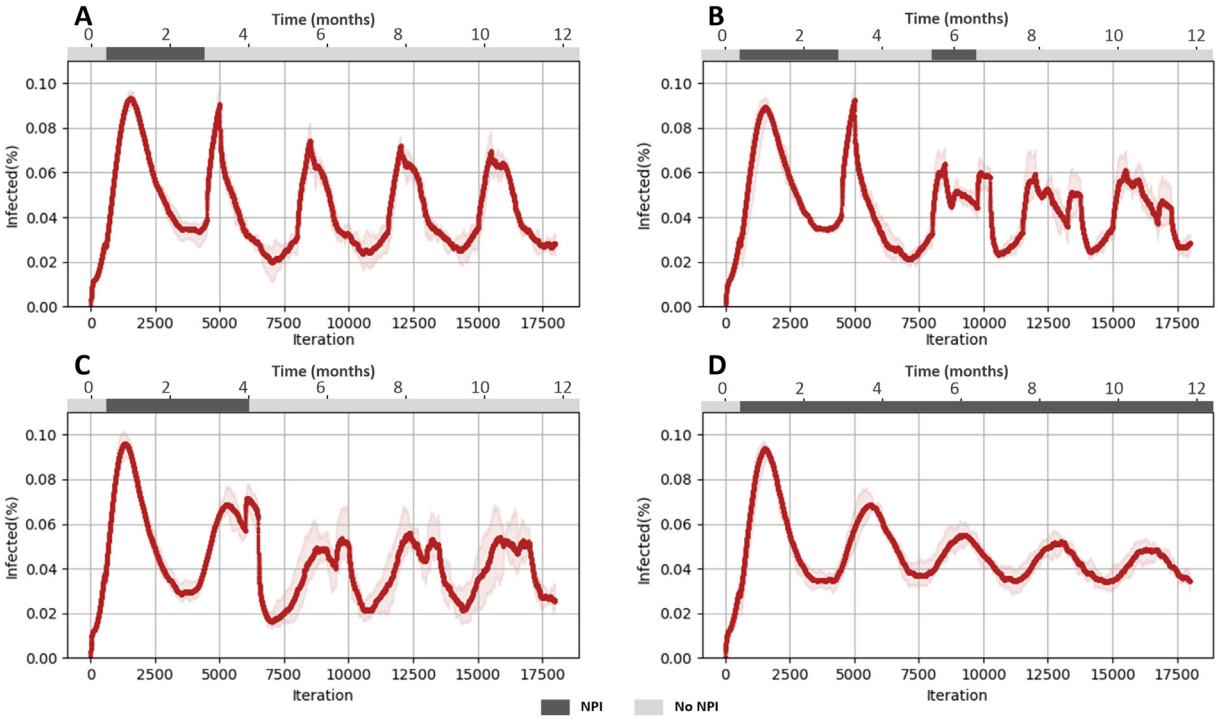


**Fig. 12.** Effect of the duration of NPIs adoption on infectious disease propagation. NPIs are assumed to be adopted during the first three months (A), the first three months as well as months 5.5 to 6.5 (B), the first four months (C), or all the time (D).

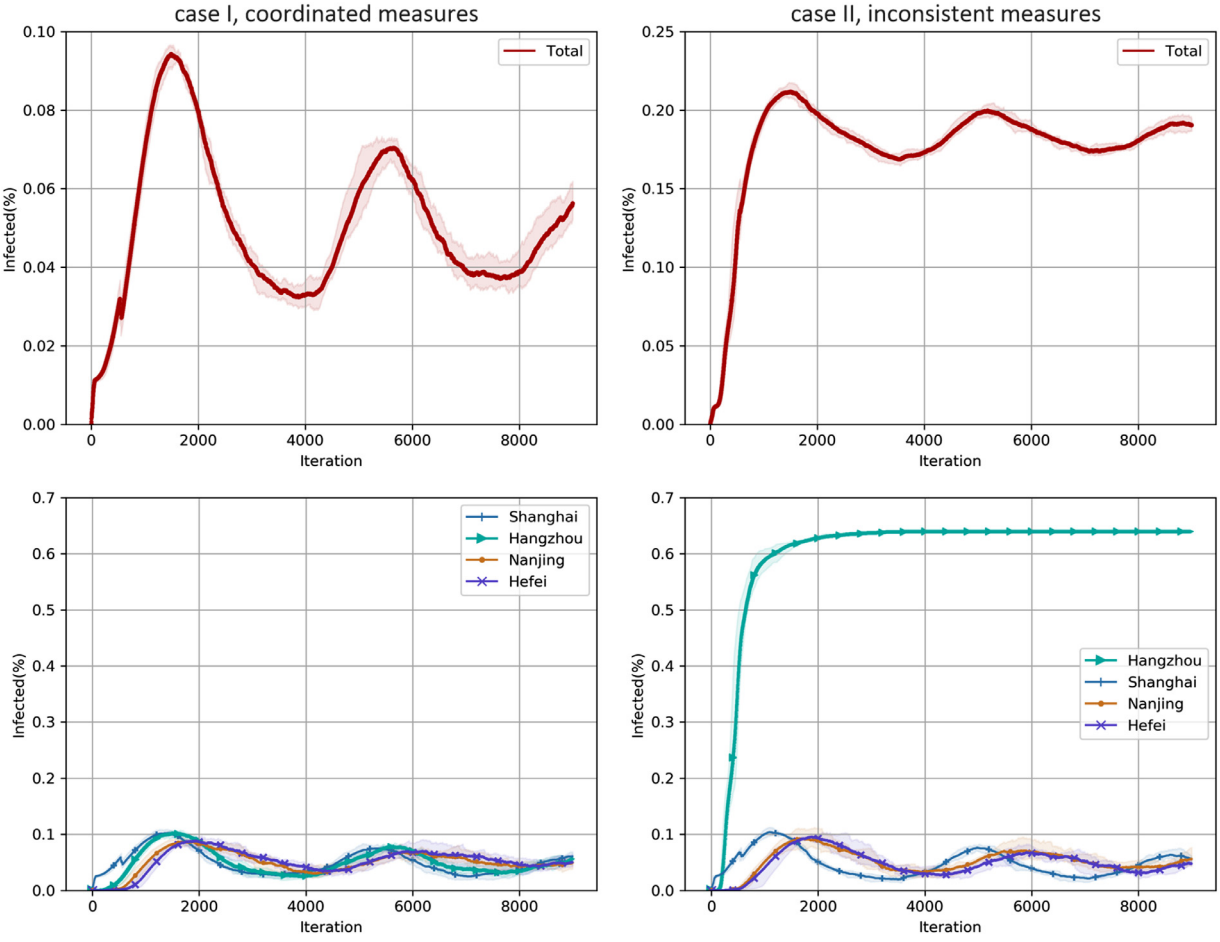


**Fig. 13.** Infectious disease transmission with coordinated and inconsistent measures. In Case I, the four cities implement coordinated public health interventions. While in Case II, the measures in Hangzhou are not as strict as that in the other three cities.

Application of the model to COVID-19 and several hypothetical scenarios illustrates the model's utility. The results show that time to the rapid growth of infections is positively correlated with the index of population inflow from the city where the disease starts. The infections will be contained if patients and the close contacts are isolated or quarantined before 30% of people in a community are infected by the virus. The duration of immunity is set to 2 months in our simulations in order to facilitate calculations, shorter than the duration in the real world (6 months or longer), which leads to more frequent outbreaks of the epidemic in the paper. Our results highlight the necessity of controlling the source of infection even if the vaccine is available. With 80% vaccination rate the peak of infections declines by 67.37%, compared to a drop of 89.56% when isolation and quarantine measures are in place. The adoption of NPIs decreases the risk of disease transmission particularly when NPIs are implemented continuously. The analysis of inconsistent interventions demonstrates the importance of regional coordination. Easing measures in one city will not only cause a significant increase in the number of infection in this city, but also worsen the situation in other cities. This model can provide quantified theoretical references to public health decision makers for minimizing the disease spread. By considering the effects that interventions and vaccination have on disease transmission, governments can make more-informed decisions about how to control the epidemic.

## Declaration of Competing Interest

The authors declare that they have no known competing financial interests or personal relationships that could have appeared to influence the work reported in this paper.

## Acknowledgments

This work is supported by National Key R&D Program of China (No. 2020YFA0714500), National Science Foundation of China (Grant nos. 72174099, 72042010), and High-tech Discipline Construction Fundings for Universities in Beijing (Safety Science and Engineering ).

## References

[1] Wikipedia, COVID-19 pandemic, 2021, (https://en.wikipedia.org/wiki/COVID-19_pandemic).
[2] Y. Niu, Z. Li, L. Meng, S. Wang, Z. Zhao, T. Song, J. Lu, T. Chen, Q. Li, X. Zou, The collaboration between infectious disease modeling and public health decision-making based on the COVID-19, J. Saf. Sci. Resil. 2 (2) (2021) 69–76.
[3] F.M. Khan, R. Gupta, ARIMA and NAR based prediction model for time series analysis of COVID-19 cases in India, J. Saf. Sci. Resil. 1 (1) (2020) 12–18.
[4] H. Tian, Y. Liu, Y. Li, C.-H. Wu, B. Chen, M.U. Kraemer, B. Li, J. Cai, B. Xu, Q. Yang, et al., An investigation of transmission control measures during the first 50 days of the COVID-19 epidemic in China, Science 368 (6491) (2020) 638–642.
[5] H.S. Badr, H. Du, M. Marshall, E. Dong, M.M. Squire, L.M. Gardner, Association between mobility patterns and COVID-19transmission in the usa: a mathematical modelling study, Lancet Infect. Dis. 20 (11) (2020) 1247–1254.
[6] W.O. Kermack, A.G. McKendrick, Contributions to the mathematical theory of epidemics. II.The problem of endemicity, Proc. R. Soc. Lond. Ser. A 138 (834) (1932) 55–83.
[7] J. Arino, C.C. McCluskey, P. van den Driessche, Global results for an epidemic model with vaccination that exhibits backward bifurcation, SIAM J. Appl. Math. 64 (1) (2003) 260–276.
[8] A. Tiwari, Modelling and analysis of COVID-19 epidemic in India, J. Saf. Sci. Resil. 1 (2) (2020) 135–140.
[9] B. Tang, F. Xia, S. Tang, N.L. Bragazzi, Q. Li, X. Sun, J. Liang, Y. Xiao, J. Wu, The effectiveness of quarantine and isolation determine the trend of the COVID-19 epidemics in the final phase of the current outbreak in China, Int. J. Infect. Dis. 95 (2020) 288–293.
[10] Y. Zeng, X. Guo, Q. Deng, S. Luo, H. Zhang, Forecasting of COVID-19: spread with dynamic transmission rate, J. Saf. Sci. Resil. 1 (2) (2020) 91–96.
[11] D. Knipl, A new approach for designing disease intervention strategies in metapopulation models, J. Biol. Dyn. 10 (1) (2016) 71–94.
[12] P.S. Peixoto, D. Marcondes, C. Peixoto, S.M. Oliva, Modeling future spread of infections via mobile geolocation data and population dynamics. An application to COVID-19 in Brazil, PLoS One 15 (7) (2020) e0235732.
[13] G. Chowell, L. Sattenspiel, S. Bansal, C. Viboud, Mathematical models to characterize early epidemic growth: a review, Phys. Life Rev. 18 (2016) 66–97.
[14] F. Lorig, E. Johansson, P. Davidsson, et al., Agent-based social simulation of the COVID-19pandemic: a systematic review, J. Artif. Soc. Soc. Simul. 24 (3) (2021) 1–5.
[15] A. Bouchnita, A. Jebrane, A hybrid multi-scale model of COVID-19 transmission dynamics to assess the potential of non-pharmaceutical interventions, Chaos Solitons Fractals (2020) 109941.
[16] P.C. Silva, P.V. Batista, H.S. Lima, M.A. Alves, F.G. Guimarães, R.C. Silva, COVID-ABS: an agent-based model of COVID-19 epidemic to simulate health and economic effects of social distancing interventions, Chaos Solitons Fractals 139 (2020) 110088.
[17] E. Cuevas, An agent-based model to evaluate the COVID-19transmission risks in facilities, Comput. Biol. Med. 121 (2020) 103827.
[18] Q. Huang, A. Mondal, X. Jiang, M.A. Horn, F. Fan, P. Fu, X. Wang, H. Zhao, M. Ndeffo-Mbah, D. Gurarie, SARS-CoV-2 transmission and control in a hospital setting: an individual-based modelling study, R. Soc. Open Sci. 8 (3) (2021) 201895.
[19] J. Swanson, A. Jeanes, Infection control in the community: a pragmatic approach, Br. J. Community Nurs. 16 (6) (2011) 282–288.
[20] CDC, Quarantine and isolation, 2021, (https://www.cdc.gov/quarantine/index.html).
[21] A. Juliani, V.-P. Berges, E. Teng, A. Cohen, J. Harper, C. Elion, C. Goy, Y. Gao, H. Henry, M. Mattar, et al., Unity: a general platform for intelligent agents, arXiv preprint arXiv:1809.02627(2018).
[22] NBSC, China statistical yearbook, 2019, (http://www.stats.gov.cn/english/Statisticaldata/AnnualData/).
[23] Baidu, Baidu migration platform, 2020, (https://qianxi.baidu.com/2020/).
[24] Sohu, Statistics of commuting distance for the normal commuters in China, 2015, (http://news.sohu.com/20150128/n408124940.shtml).
[25] B.J. Mohler, W.B. Thompson, S.H. Creem-Regehr, H.L. Pick, W.H. Warren, Visual flow influences gait transition speed and preferred walking speed, Exp. Brain Res. 181 (2) (2007) 221–228.
[26] K. Wan, J. Chen, C. Lu, L. Dong, Z. Wu, L. Zhang, When will the battle against novel coronavirus end in Wuhan: a SEIR modeling analysis, J. Global Health 10 (1) (2020) 011002.
[27] L. Luo, D. Liu, X.-l. Liao, et al., Modes of contact and risk of transmission in covid-19: a prospective cohort study 4950 close contact persons in guangzhou of, China (2020).
[28] S. Ying, F. Li, X. Geng, Z. Li, X. Du, H. Chen, S. Chen, M. Zhang, Z. Shao, Y. Wu, et al., Spread and control of COVID-19 in China and their associations with population movement, public health emergency measures, and medical resources, medRxiv (2020).
[29] J.I. Cohen, P.D. Burbelo, Reinfection with SARS-CoV-2: implications for vaccines, Clin. Infect. Dis. (2020).
[30] J. Rothwell, Americans' social contacts during the COVID-19 pandemic, 2020, (https://news.gallup.com/opinion/gallup/308444/americans-social-contacts-during-covid-pandemic.aspx).
[31] Marco D'Orazio, Gabriele Bernardini, Enrico Quagliarini, A probabilistic model to evaluate the effectiveness of main solutions to COVID-19 spreading in university buildings according to proximity and time-based consolidated criteria, Building simulation 14 (6) (2021) 1795–1809.